The Effect of Ladle Furnace Slag (LFS) Content Replacement as a Supplementary Cementitious Material in Portland Cement-Based Systems

Paulo Araos(✉), Anna Uribarri, Marilda Barra, and Diego Aponte

Universitat Politècnica de Catalunya Barcelona TECH, 08034 Barcelona, Spain
paulo.sebastian.araos@upc.edu

Abstract. Portland cement (OPC) and steelmaking industries exhibit high production levels and are expected to continue in the near future. Their industrial processes are not considered environmentally friendly and are estimated to be responsible for 4–7% of worldwide CO_2 emissions. To mitigate their negative externalities, they introduce several improvements in their processes. The steelmaking industry generates a large volume of solid waste, mainly slags. Electric arc furnace slag (EAFS) and ladle furnace slag (LFS) shows exciting properties to be used as construction material. Currently, only EAFS is valorized, mainly as a granular material for different pavement layers. Instead, LFS presents technological barriers (low cementing activity and expansive problems) that prevent them from being valorized and finally deposited in landfills. This work explores a safe/high-value application for LFS as a supplementary cementitious material (SCM). Pastes/mortars were produced to study the effect of varying the LFS-content replacement. Chemical/mineralogical characterization of raw/hydrated samples and fresh/hardened state properties were tested at different ages to study the physical-mechanical performance and microstructure evolution. Our results suggest that LFS has good potential as SCM, modifying the fresh/hardened performance depending on LFS content: by decreasing workability, accelerating the setting time, and lowering the strength. Also, it increases the potential volumetric instability issues. The compressive strength gap decreases with time, reaching over 30 MPa for 25/50 wt% replacements at 28–98 days. Finally, the microstructure evolution shows a shift in the typical OPC hydration reactions, producing higher AFm-AFt products due to the higher calcium-aluminates reactive phases in the slag.

Keywords: Ladle furnace slag · Portland cement · supplementary cementitious material · compressive strength · microstructure

1 Introduction

Cement and steelmaking industries, both major actors in the construction sector, exhibit a continuous increase in their production levels and, according to recent studies, will keep growing in the near future [1]. Nonetheless, their industrial processes are not considered environmental-friendly. They are very intensive in natural resource consumption

A. Jędrzejewska et al. (Eds.): SynerCrete 2023, RILEM Bookseries 44, pp. 76–87, 2023.
https://doi.org/10.1007/978-3-031-33187-9_8

and generate considerable amounts of greenhouse gas emissions, approximately 4–7% of CO_2 worldwide [2]. In both cases, numerous improvements have been introduced throughout the entire value chain to mitigate these negative externalities [2–5].

The steelmaking process generally comes from two main production routes, iron ore-based steelmaking (IO-BS) and scrap-based steelmaking (S-BS), with a world distribution production of 70%-30%, respectively. Although, future trends seem to favour the second one due to lower energy consumption and the possibility of reusing metal scrap [1, 6]. The S-BS route generates large amounts of solid wastes such as the electric arc furnace slag (EAFS) and ladle furnace slag (LFS) [7, 8]. It is well known that for every ton of steel produced, on average, 110–150 kg of EAFS and 20–30 kg of LFS are generated [9]. Both slags display attractive physical properties, chemical-mineralogical composition, and affinity with cement-based materials that postulated them to be part of the next generation of green-building materials [10].

Currently, only EAFS is valorized, primarily as aggregates in road-pavement construction (sub-base, base, and surface layers). However, due to technological barriers in its valorization process (low cementing activity/strength gain and volume instability issues), LFS's final destination is to be deposited in landfills [10]. These technological barriers depend mostly on the LFS mineralogical composition, especially with the absence/low content of reactive calcium silicates, the presence of free-CaO, periclase, and highly reactive calcium-aluminates phases. Once incorporated into a rigid matrix, they could experience expansive reactions or a series of metastable phase transformations when hydrated, contributing to instability problems and low strength [11–14].

So far, several works have studied the use of LFS as supplementary cementitious material (SCM), studying the effect of different slag/dossage parameters mostly on fresh/hardened state properties and durability tests, using low to medium LFS-content replacements (from 5wt% to 30wt%), obtaining contradictory results [15–20]. These performance differences are mainly associated with the high variability of chemical/mineralogical composition (even in the same plant), the wide range of particle size distribution (PSD) between different slags, and the non-comparable mixing proportions.

This work explores a safe and high-value application to valorize the use of LFS as an SCM, reduce Portland cement (OPC) consumption, and mitigate the negative externalities of cement and steelmaking industries. The main objective is to study the effect of different LFS-content replacements (from medium to high wt%) over the early hydration reactions and fresh/hardened state properties, focusing on the physico-mechanical performance and volumetric instability issues in an OPC-mortar matrix. Finally, identify the microstructure evolution and correlate this with the macro properties performance.

2 Materials and Methods

2.1 Materials

The materials used in this study were a Portland cement type I 52.5 R (CEM) according to UNE-EN 197-1 [21], composed mostly of clinker and minor phases such as gypsum and limestone. Tap water (W) and limestone aggregate with all particles below 4 mm (F-Ag).

A Spanish ladle furnace slag (LFS-A) with all particle sizes below 0.045 mm and a density of 2.9 g/cm^3, according to UNE 80103:2013 [22]. The chemical composition results show that cement and LFS-A presented similar chemical compositions for the major oxides. Both samples were rich in Ca and Si and, to a minor extent, in Fe, Al, and Mg (representing more than 95% and 83% of the total mass in cement and slag, respectively). Smaller amounts of S, Mn, and traces of other elements were found. The main physical properties and chemical composition of the raw materials are shown in Table 1 and Table 2, respectively.

Table 1. Physical properties of raw materials.

Material	Density [g/cm^3]	SSA [m^2/g]	D10 [um]	D50 [um]	D90 [um]
CEM	3.2	0.9	3.0	14.3	35.7
LFS-A	2.9	1.4	1.9	10.2	26.1
F-Ag	2.7	-	-	-	-

The LFS-A mineralogical composition is composed of silicates and aluminates of calcium and magnesium, including reactive phases with hydraulic/expansive activity and non-reactive phases that could act as filler, such as β-C_2S, mayenite, periclase, portlandite, brucite, calcite, γ-C_2S, gehlenite, merwinite, and wüstite. It is important to highlight the absence of free-CaO, also the presence of periclase, β-C_2S, and mayenite. The first two phases are problematic as they are the main responsible phases that could produce volumetric instability issues. The latter two gave the slag cementing activity and could produce a faster setting in the case of mayenite. The LFS chemical/mineralogical composition is in agreement with the literature [3–7].

Table 2. Chemical composition of raw materials (in %).

Oxides	CaO	SiO_2	Al_2O_3	Fe_2O_3	MgO	SO_3	∑others	LOI
CEM	63.3	18.7	4.7	3.3	1.5	3.1	1.5	2.6
LFS-A	41.5	25.5	5.8	4.3	5.5	2.6	2.0	12.8
F-Ag	54.3	0.9	1.1	0.2	0.6	0.1	0.1	42.7

2.2 Mix Design and Sample Preparation

To study the effects of different slag content replacement as an SCM, mortar samples were made using 25wt%, 50wt%, and 75wt% LFS-A cement replacement. A water-to-cementitious material (cement + slag) ratio (W/CM) of 0.5 was selected, and a 3:1 sand-to-cementitious material was used. The proposed mixtures for LFS-A cement replacement (M-LFS-A-25, M-LFS-A-50, and M-LFS-A-75, respectively) are shown

in Table 3. Sample CPC corresponds to the control sample using only Portland cement as the cementitious material without any slag addition.

The process described in UNE-EN-196-1 [23] was used to prepare the mortar batches. After being prepared, the mixtures were poured into prismatic oiled molds (4x4x16 cm^3 for the physical-mechanical test and 2.5 × 2.5 × 28.5 cm^3 for the volumetric instability test). For each batch, four molds were prepared for physical-mechanical tests and two for the volumetric instability test (each mold contains three prismatic specimens and two prismatic specimens, respectively). All samples for the physical-mechanical test were cured inside a humidity chamber (95% relative humidity and 20 °C) until tested. The volumetric instability specimens were cured for one week inside the humidity chamber and then subjected to 2 types of curing environments: i) kept in the humidity chamber (labeled HC); ii) submerged in water inside a sealed container in an oven at 70 °C (labeled SW).

Table 3. The proposed dosage of the mortar samples (in grams).

Sample	Cement	Water	Aggregates	LFS
Control	450	225	1350	-
M-LFS-A-25	337.5	225	1350	112.5
M-LFS-A-50	225	225	1350	225
M-LFS-A-75	112.5	225	1350	337.5

2.3 Testing Procedures

A complete study of the raw material chemical/mineralogical composition and characterization of the LFS-cement matrix microstructure evolution was carried out. X-ray fluorescence (XRF) and X-ray diffraction (XRD) techniques were used. Cement pastes with similar proportions to the mortar samples were made to study the microstructure evolution at 7, 28, and 98 days. The hydration of the specimens was stopped with the solvent exchange method. Then the samples were pulverized to a particle size below 0.063 mm, homogenized, and ready to use in the aforementioned techniques.

The chemical composition was determined by XRF measurements using a Philips spectrometer, model PW2400. The mineralogical composition was determined by XRD measurements using a Philips X-ray diffractometer with a Panalytical X'Pert PRO MPD Alpha 1 diffractometer using Cu Kα radiation ($\lambda = 1.5406$ Å, 45 kV–40 mA). The scans were performed between 5°2θ and 65°2θ with a 0.019° step size and a counting time of 0.8 s per step. The qualitative identification of all phases was performed with Panalytical X'Pert HighScore Plus software with PDF-2 and COD databases.

The initial hydration reactions of cement paste with different LFS content replacements were studied with semi-adiabatic calorimetry tests conducted for 150 h. The experimental setup consists of an SQ2020 squirrel datalogger (Grant Instrument) connected to five type K thermocouples. Four thermocouples were inserted into fresh, recently mixed

paste samples poured into a sealed plastic vessel and one into a control water sample. The plastic vessels were immediately placed inside an insulated recipient and finally put into an expanded polystyrene container with a capacity of five samples. External hand-mixing for 1.5 min was conducted, and the room temperature was approximately 25 °C.

To study the effect of LFS content replacement as an SCM at the macroscopic level, fresh/hardened state properties were measured, such as: setting time according to UNE-EN-196-3 [24], flow table test according to UNE-EN-12350-5 [25], density, absorption, and pore volume were determined according to ASTM C642 [26], flexural/compressive strength according to UNE-EN-196-1 at 7, 28, and 98 curing days. Volumetric instability was measured according to ASTM C490-04 [27] and ASTM C1038 [28] exposed to 2 types of curing environments (HC and SW described in Sect. 2.2). For the hardened-state properties, the results correspond to an average of: 3 samples in physical-mechanical tests (for each age), and 2 samples in the volume instability test for each measure.

3 Results and Discussion

3.1 Early Hydration Reactions and Fresh-State Properties

Figure 1a shows the early hydration reactions of all paste samples. The Portland cement early hydration process is dominated by the hydration of the silicate phases and consists of two main exothermic processes. In the first minutes, a steep temperature increase peak appears associated with the dissolution of aluminate/silicate phases releasing Al, Ca, and Si into the system. And the formation of ettringite due to the hydration of the highly reactive aluminates phases present in the cement (C3A). Then for a few hours, the sample enters a dormant period just before the early reactive silicate phases in cement (C3S) start to contribute to the hydration process and appears as the main/maximum exothermic peak associated with the initial formation of the amorphous CSH gel and crystalline portlandite.

The blended LFS-cement samples observed a change in the early hydration behavior with a dependency on LFS-content replacement. The initial dissolution/aluminate peak intensity increases, and the main silicate peak intensity decrease and appears to be delayed as the LFS-content replacement increases. With a 25wt% LFS-content replacement, the curve was very similar to the control sample due to the cement dilution effect, indicating that the OPC hydration process still governs the early hydration reactions (involving cement and slag phases). When the LFS-content replacement increases to 50wt%, the silicate peak intensity decreases dramatically, the delay in its formation continues and the dilution/aluminate peak intensity increase, reaching very similar maximum values to the second peak. This could indicate that the aluminates in the slag (mayenite) start affecting the early hydration reactions. Finally, with a 75wt% LFS-content replacement, the trend changed completely. The silicate peak intensity continues to decrease and delay its formation. Also, the silicate dilution/aluminate maximum intensity peak surpasses the second exothermic peak. This could indicate that the aluminates in the system take over the early hydration reactions, and the LFS-A hydration process starts to govern the early hydration reactions.

Figure 1b shows the flow table test results, where it can be observed that the LFS-mortar samples exhibit a decrease in the flow table consistency with an LFS-content dependency. The higher the LFS-cement replacement, the lower the consistency of the sample. This behavior change could be related to the contribution of mayenite with the LFS-content replacements in the samples, which produce an acceleration of the early hydration reactions (as described previously). Promoting the formation of aluminates-hydration products that could provide the samples with a fast setting and early hardening properties.

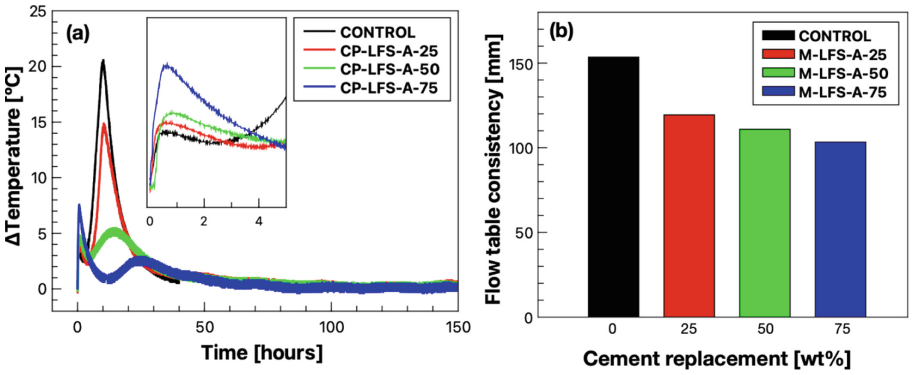

Fig. 1. Early hydration reactions and fresh state property test: (a) Semi-adiabatic calorimetry (b) Flow table consistency.

3.2 Microstructural Characterization of LFS-Cement Hydrated Systems

Figure 2 and Fig. 3 show the XRD scans of the raw materials (cement and LFS-A) and hydrated blended cement samples (Control, M-LFS-A-25, M-LFS-A-50, and M-LFS-A-75) at 7 and 98 days, respectively. All samples exhibit a similar mineralogical composition, mainly a mixture of phases present in the raw materials (cement and LFS-A), with a dilution effect of cement/slag phases depending on the LFS-content replacement. Finally, characteristic peaks of slow/non-reactive cement/slag phases are still visible after 98 curing days.

The microstructural evolution exhibit a dependency on the LFS-content replacement, where at seven days (see Fig. 2), it is clearly observed the consumption of reactive phases of cement and LFS-A such as C_3S, C_3A, gypsum, mayenite, β-C_2S, and a calcium-aluminium hydrate type phase (C·A·H). Also, the formation of characteristic products in an OPC matrix, like portlandite, calcite, and a kind of baseline displacement as a hump between 25º2θ to 40º2θ typical of the C-S-H type gel formed during the hydration reactions of these LFS-cement systems. All samples display a low ettringite (AFt) formation but started to show an AFm-type phase formation called monocarboaluminate (AFm-CO_3). Possibly due to an AFt to AFm type phase transformation with a high calcite content in the system. At this time, it is also observed a lower formation of portlandite and lower consumption of cement silicate phases (C_3S) as the LFS-content

replacement increase. These could indicate a lower degree of hydration, possibly due to the cement dilution effect and a change in the early reactions that favor the hydration of aluminates over silicates.

As time passes and the hydration reactions continue (see Fig. 3), all samples at 98 curing days exhibit a decrease in the reactive cement/slag phases (C_3S, C_3A, β-C_2S), together with the total consumption of gypsum indicating that the degree of hydration increased. Furthermore, it is clearly observed the formation of AFt/AFm-CO_3 phases with an LFS-content replacement dependency. The control sample shows very little AFt to AFm-CO_3 transformation.

As the LFS-content replacement increase (25wt%), the AFm-CO_3 peaks appears more clearly. But this transformation is modified when the LFS-content replacement continues to increase (50wt% and 75wt%). A lower resolution of the AFm-CO_3 peaks is observed, which is associated with a less crystalline phase and appears to be the formation of newer AFm-type phases like hemicarbonate (AFm-0.5CO_3). This change in the LFS-cement systems hydration products may be possible due to the increasingly higher content of calcite and aluminates added in the slag, which alters the normal OPC reactions accelerating the AFt to AFm transformation. Finally, periclase consumption is evident in all the blended LFS samples between 7 to 98 days as the intensity of its main peaks decreases.

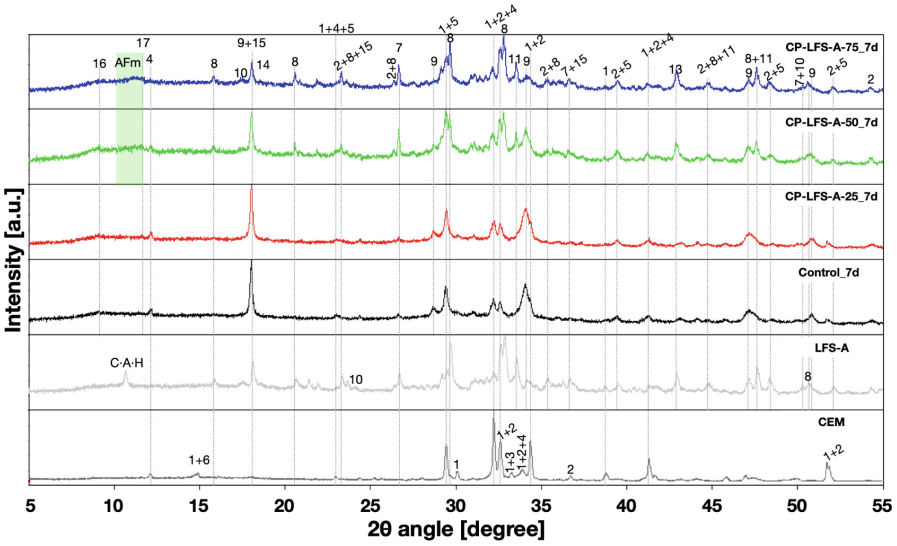

Fig. 2. XRD diffract grams of raw and hydrated samples at seven curing days, where: (1) C_3S; (2) β-C_2S; (3) C_3A; (4) C_4AF; (5) calcite; (6) gypsum; (7) quartz; (8) γ-C_2S; (9) portlandite; (10) gehlenite; (13) periclase; (14) brucite; (15) mayenite; (16) AFt; (17) AFm-CO_3.

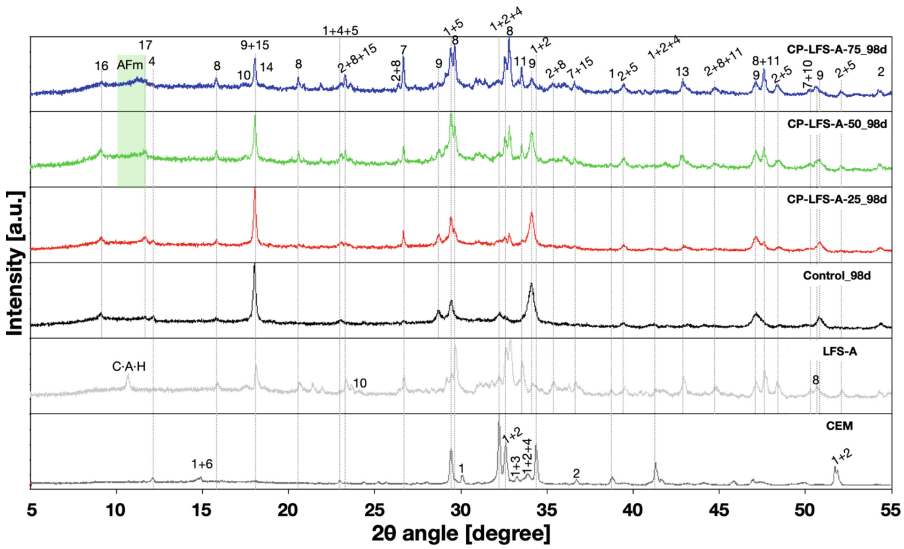

Fig. 3. XRD diffractograms of raw and hydrated samples at 98 curing days, where: (1) C_3S; (2) β-C_2S; (3) C_3A; (4) C_4AF; (5) calcite; (6) gypsum; (7) quartz; (8) γ-C_2S; (9) portlandite; (10) gehlenite; (13) periclase; (14) brucite; (15) mayenite; (16) AFt; (17) AFm-CO_3.

3.3 Evolution of Physical-Mechanical Properties

The evolution of physical properties studied in this work for all the mortars can be seen in Fig. 4. Figure 4a shows the measured densities as a function of curing time. All samples displayed similar behavior, the density increases as time passes, and the values are in the expected range (2.0–2.2 g/cm^3). The control sample has the highest density at all ages and the LFS-mortar samples density decrease with the increase of LFS-content replacement. Instead, Fig. 4b shows the porosity results as a function of curing time, which exhibits the opposite trend. The porosity decreases as time passes. Also, the control sample has the lowest pore volume, while the LFS-mortar sample's pore volume increases with LFS-content replacement. This behavior is expected due to the cement dilution effect, the lower density of LFS-A than cement (see Table 2), and the evolution of cement-LFS hydration reactions. The recently formed phases have a larger volume than the anhydrous phases, occupying the free space available in the system and densifying the mortar matrix.

Figure 5 shows the mechanical performance evolution of all the samples at 7, 28, and 98 curing days, showing a quick strength gain at early ages (from 7 to 28 days) with a later rate reduction (from 28 to 98 days). The control sample obtained the best mechanical performance in compressive and flexural strength, reaching values of 63.2 and 11.5 MPa at 98 curing days, respectively (see Table 4). The LFS-content replacements samples show a decrease in mechanical performance compared to the control sample (see Fig. 5a and Fig. 5b) with an LFS-content dependency. The higher the LFS-cement replacement, the lower the mechanical performance of the sample, primarily due to the cement dilution effect that is caused by decreasing the cement content in the mortars with the increasing

LFS-content replacement and the lower cementing activity of the LFS provided by the hydration of β-C_2S and mayenite present in the slag. All LFS-mortar samples show a similar evolution trend. At early ages, the compressive index performance is below the LFS-content replacement, indicating that only the OPC hydration process contributes to the strength gain, and the input of LFS is very low at this time.

Table 4. Mechanical performance index compared to control sample.

Age [days]	Control strength [MPa]		Index performance [%]		
	Compressive	Flexural	25wt%	50wt%	75wt%
7	51.1	8.6	73/85	46/74	3/9
28	58.7	11.0	75/81	52/61	18/34
98	63.2	11.5	80/75	54/61	25/45

* X / Y, where X corresponds to the compressive index performance (PI_C), and Y corresponds to the flexural index performance (PI_F).

As time passes, the compressive index performance increases, surpassing the LFS-content replacement in samples 25wt% and 50wt%. This could be related to a mix-contribution of OPC and LFS-A, where the β-C_2S phase in cement and LFS-A begins to hydrate and contributes to strength gaining. Finally, it can be observed that the 75wt% sample show very low mechanical performance at early ages, associated with a change in the strength gain contribution. At this time, mainly the aluminates (C_3A/mayenite and gypsum) present in both cement and slag were the active phases and, to a lesser extent, the C_3S in cement. Then similar to the 25wt% and 50wt% samples, as time passes, a mix-contribution of OPC and LFS-A occurs, increasing the mechanical performance of the sample.

3.4 Volumetric Instability

Figure 6 shows the volumetric instability behavior of mortar samples up to 135 curing days in two curing environments (HC and SW). As shown in Fig. 6a (HC environment 95% H.R. and 22ºC), all samples display a slight expansive trend, reaching similar expansion values between 0.003% and 0.007%. This behavior could be associated with the swelling effect produced in the HC environment that presents ideal conditions for hydration with a continuous moisture gain and limited evaporation, avoiding any shrinkage and producing a volume increase. In Fig. 6b, the SW environment, due to the acceleration of the reactions, all samples exhibit a higher expansion trend compared to the HC environment. Also, the LFS-mortar samples differentiate them from the control sample (approximately 0.03% linear expansion), reaching expansion values between 0.05% to 0.06%. This behavior difference exhibits a slight LFS-content dependency where the 25wt% and 50wt% samples present similar results, but the 75wt% cement replacement increases the linear expansion. This tendency could be associated with activating the remaining phases with hydraulic and expansive behavior in the slag (β-C_2S, mayenite, and periclase) that overcame the cement dilution effect.

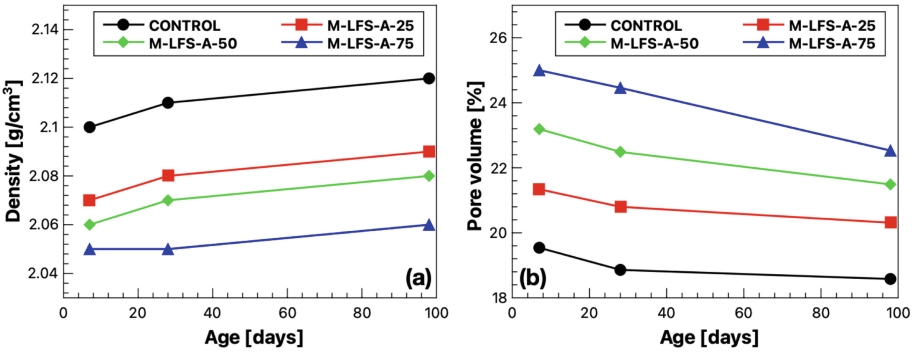

Fig. 4. Physical properties of the LFS mortar samples.

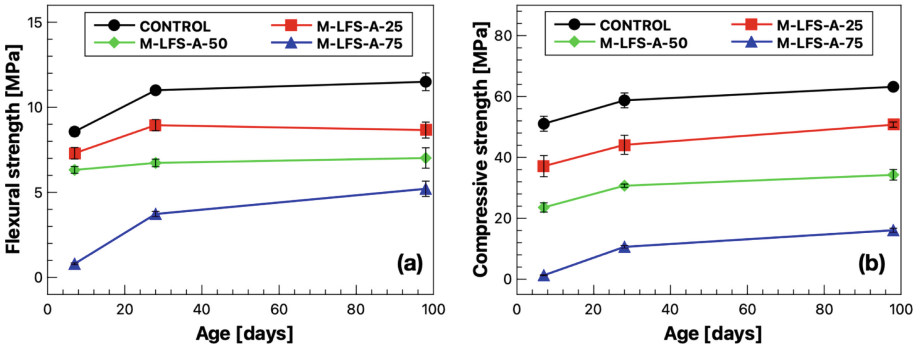

Fig. 5. Mechanical properties of the LFS mortar samples.

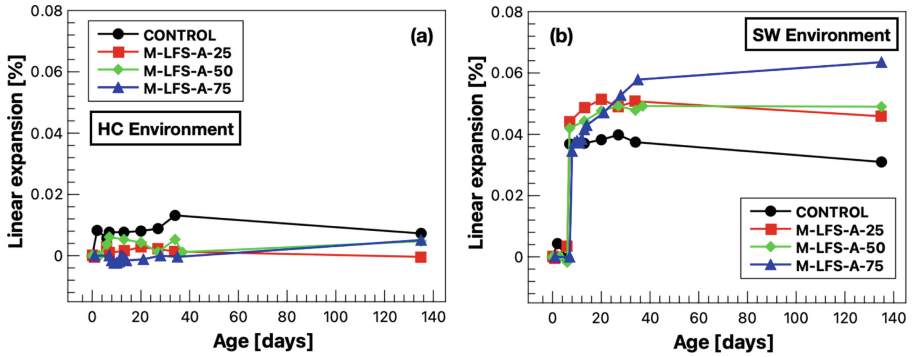

Fig. 6. Volumetric instability evolution of the LFS mortar samples.

4 Conclusions

In the present work, extensive experimental research was conducted to characterize the microstructure/macrostructural performance of LFS-cement systems, suggesting that LFS could be used as an SCM in medium to high cement replacement. This could be very beneficial from an environmental point of view, reducing cement usage and valorizing LFS, a waste from the steelmaking industry.

LFS-mortar samples display a lower mechanical performance than the control sample with an inverse dependency on the LFS-content replacement, mainly due to the cement dilution effect and lower cementing activity of the slag. At early ages appears to be a minor input of the slag to strength gain. As time passes, the slow reactive phases in the slag with cementing activity start contributing to the strength gain and reaching non-negligible compressive strength values over 30 MPa at 98 curing days for 25wt% and 50wt% LFS-content replacement.

LFS-mortar samples display an increase in potential volume instability performance compared to the control sample, with a direct dependency on LFS-content replacement and type of curing environment. In optimal curing conditions, all samples exhibit similar behavior. In an accelerated curing environment, the LFS-mortar samples display higher expansive values than the control sample. Possibly, due to the activation of slow reactive phases present in the slag (periclase) or to the higher content of aluminates with delayed hydration (AFt/AFm type phases).

The early hydration reactions and fresh state properties are directly affected by the LFS-content replacement due to the incorporation of highly reactive aluminate phases within the slag. At smaller LFS concentrations exists only a cement dilution effect, but as the LFS-content replacement increases, it displays a change in the behavior. Accelerating the early aluminate-phases reactions and delaying the silicate-phase reactions, producing an increase in the early heat release, and decreasing the workability.

The mineralogical composition of the slag is a critical factor that influence the fresh/hardened state properties of the LFS-cement system. The aluminate-phases are determinant in the early hydration reactions/workability, the reactive silicate-phases to the strength gain, and finally in the absence of free-CaO periclase would be the main responsible for the expansive reactions.

References

1. Pauliuk, S., et al.: The steel scrap age. Environ. Sci. Technol. **47**(7), 3448–3454 (2013)
2. Schneider, M.: The cement industry on the way to a low-carbon future. Cem. Concr. Res. **124**, 105792 (2019)
3. Madlool, N.A., et al.: An overview of energy savings measures for cement industries. Renew. Sustain. Energy Rev. **19**, 18–29 (2013)
4. Lothenbach, B., Scrivener, K., Hooton, R.D.: Supplementary cementitious materials. Cem. Concr. Res. **41**(12), 1244–1256 (2011)
5. Thomas, M.: Supplementary Cementing Materials in Concrete, 1st edn. CRC Press, Boca Raton (2013)
6. Morfeldt, J., Nijs, W., Silveira, S.: The impact of climate targets on future steel production - an analysis based on a global energy system model. J. Clean. Prod. **103**, 469–482 (2015)

7. Jiang, Y., et al.: Characteristics of steel slags and their use in cement and concrete - a review. Resour. Conserv. Recycl. **136**, 187–197 (2018)
8. Zhao, J., Yan, P., Wang, D.: Research on mineral characteristics of converter steel slag and its comprehensive utilization of internal and external recycle. J. Clean. Prod. **156**, 50–61 (2017)
9. Shi, C.: Steel slag—its production, processing, characteristics, and cementitious properties. J. Mater. Civ. Eng. **16**, 230–236 (2004)
10. Montenegro-Cooper, J.M., et al.: Study of the expansive behavior of ladle furnace slag and its mixture with low quality natural soils. Constr. Build. Mater. **203**, 201–209 (2019)
11. Ranfionich, E.V., Barra, M.: Reactividad y expansión de las escorias de acería de horno de arco eléctrico en relación con sus aplicaciones en la construcción. Materiales de Construcción CSIC **51**(263–264), 137–148 (2001)
12. Setién, J., Hernández, D., González, J.J.: Characterization of ladle furnace basic slag for use as a construction material. Constr. Build. Mater. **23**, 1788–1794 (2009)
13. Yildirim, I.Z., Prezzi, M.: Chemical, mineralogical, and morphological properties of steel slag. Adv. Civil Eng. **2011**, 463638 (2011)
14. Montenegro, J.M., et al.: Ladle furnace slag in the construction of embankments: expansive behavior. J. Mater. Civ. Eng. **25**, 972–979 (2013)
15. Wang, Y., Suraneni, P.: Experimental methods to determine the feasibility of steel slags as supplementary cementitious materials. Constr. Build. Mater. **204**, 458–467 (2019)
16. Papayianni, I., Anastasiou, E.: Effect of granulometry on cementitious properties of ladle furnace slag. Cement Concr. Compos. **34**, 400–407 (2012)
17. Herrero, T., et al.: Effect of high-alumina ladle furnace slag as cement substitution in masonry mortars. Constr. Build. Mater. **123**, 404–413 (2016)
18. Fang, K., et al.: Utilization of ladle furnace slag as cement partial replacement: influences on the hydration and hardening properties of cement. Constr. Build. Mater. **299**, 124265 (2021)
19. Fang, K., et al.: Use of ladle furnace slag as supplementary cementitious material before and after modification by rapid air cooling: a comparative study of influence on the properties of blended cement paste. Constr. Build. Mater. **314**, 125434 (2022)
20. Sideris, K., et al.: Mechanical characteristics and durability of self compacting concretes produced with ladle furnace slag. Constr. Build. Mater. **170**, 660–667 (2018)
21. UNE-EN 197-1, Cement - Part 1: Composition, specifications and conformity criteria for common cements, AENOR, Madrid (2011)
22. UNE 80103: Test methods of cements. Physical analysis. Actual density determination, AENOR, Madrid (2013)
23. UNE-EN 196-1, Methods of testing cement - Part 1: Determination of strength, AENOR, Madrid (2018)
24. UNE-EN 196-3, Methods of testing cement - Part 3: Determination of setting times and soundness, AENOR, Madrid (2017)
25. UNE-EN 12350-5: Testing fresh concrete - Part 5: Flow table test, AENOR, Madrid (2020)
26. ASTM C642-13, Standard Test Method for Density, Absorption, and Voids in Hardened Concrete, ASTM International, West Conshohocken, PA (2013)
27. ASTM C490 / C490M-17, Standard Practice for Use of Apparatus for the Determination of Length Change of Hardened Cement Paste, Mortar, and Concrete, ASTM International, West Conshohocken, PA (2017)
28. ASTM C1038/C1038M-19, Standard Test Method for Expansion of Hydraulic Cement Mortar Bars Stored in Water, ASTM International, West Conshohocken, PA (2019)